DOI: 10.1016/S1872-5813(21)60009-9

The optimum conditions for methanol conversion to dimethyl ether over modified sulfated zirconia catalysts prepared by different methods

Doaa S. EL-DESOUKI[1], Amina H. IBRAHIM[1], Samira M. ABDELAZIM[1], Noha A. K. ABOUL-GHEIT[1,*], Dalia R. ABDEL-HAFIZAR[2]

(1. *Processes Development Department*, *EPRI*, *Cairo* 11727, *Egypt*; 2. *Refining Department*, *EPRI*, *Cairo* 11727, *Egypt*)

Abstract: Sulfated zirconia (SZ) and two promoted 1%Mn/SZ catalysts which have been prepared via sol gel (Mn/SZ-S) and impregnation (Mn/SZ-I) methods were studied. The morphology of the catalysts was characterized by XRD, BET, NH_3-TPD, ICP, SEM and FT-IR analysis. The conversion of methanol to dimethyl ether and hydrocarbons was carried out in the temperature range of 120−300 °C. The Mn/SZ-S showed the highest activity due to the high surface area with suitable acidity. The optimum condition of Mn/SZ-S catalyst was investigated at 200 °C and LHSV of 0.02 h^{-1} in a time range from 30 to 210 min. It was found that the total conversion decreased from 80.18% to 53.26% at 210 min. The reusability of this catalyst was studied at the optimum condition up till four cycles for 1 h. The characterization of the reused catalyst showed a significant change in the structure and surface acidity due to the blockage of the surface acid sited by carbonaceous materials.

Key words: catalysts; dehydration; DME; sulfate content; sulfated zirconia

CLC number: O643 **Document code:** A

Hydrocarbons are one of the most desirable products derived from crude oil, and with increasing concerns about the depletion of crude oil, many researchers have directed towards producing valuable products from alternative sources such as natural gas or methanol. Also methanol could be considered as a feedstock for the production of hydrocarbons and dimethyl ether (DME). DME has become one of the most promising green fuels with higher cetane number, higher ignition ability and lower combustion residues. It could be used as a replacement for CFCs that has a devastating effect on the ozone layer in the atmosphere, as well as it acts as a mediator in many processes that produce liquefied petroleum gas (LPG) and dimethyl sulfate. Methanol to hydrocarbon (MTH) involves dehydration of methanol to produce equilibrium mixture of methanol, dimethyl ether and water, then it will direct toward three different paths, MTG (Methanol-Gasoline), MTO (Methanol-Olefins) and MTA (Methanol-Aromatics). These processes were adjusted according to proper catalysts and reaction conditions.

Solid acid catalysts as zeolite were used to catalyze the reactions of MTH. Various types of acid catalysts have been studied in the dehydration of methanol such as mesoporous silicates, γ-Al_2O_3, zeolites[1−5], kaolinite[6], sulfated zirconia and TiO_2-ZrO_2. Zeolites and γ-Al_2O_3 have noticeable catalytic actions in MTH but they have shown a tendency to rapidly deactivate and low methanol dehydrating rate, in addition to that SZ was developed as a replacement for commonly used solid acid catalysts, so SZ with its super acid properties and stability have become one of the most desirable catalysts for many significant reactions such as isomerization[7], esterification[8], and alkylation at low temperatures. The acidity and performance of the SZ catalyst depend on the preparation method, surface area, zirconia source, precipitating agent, sulfate source, pH value, temperature, aging time, and the calcination temperature. SZ tends to deactivate when hydrocarbons interact on the surface. The incorporation of metal oxides has positive effects on the activity and stability of SZ: (i) that prevents the transition from a tetragonal phase to a monophasic phase; (ii) increasing active sites and enhancing the strength of surface acid sites, and (iii) extending the lifetime of the catalyst[9]. The role of Pt in SZ activity and stability has been discussed[10], as well as the development of Brønsted acid sites in the presence of Pt. Methanol conversion on Ni-ZSM-5 catalyst has increased with time, suggesting that Ni can adjust the strength of strong acid sites[11].

Received: 2020-08-28; Revised: 2020-11-05

* Corresponding author. E-mail: nohakadry3yoa@yahoo.com.

本文的英文电子版由 Elsevier 出版社在 ScienceDirect 上出版 (http://www.sciencedirect.com/science/journal/18725813)

Recently, different metal oxides (Fe_2O_3, Co_2O_3, and Ni_2O_3) were incorporated into SZ[9]. Metal oxides have an effect on the valence state of S since S^{6+} only contributes to the acidic property of the catalyst[12]. The role of transition metals on SZ have been tested for *n*-butane dehydroisomerization in many literatures. SZ promoted with Mn, Al, Ni and Cu were synthesized with Zr:*M* molar ratios of 1.0/0.1, 1/0.5 and 1.0/1.0. The presence of transition metals have improved the catalytic stability and selectivity of the catalysts[13]. Also, it was noticed that the SZ doped with 1.5% Fe and 0.5% Mn has increased the activity of unpromoted SZ by 3 orders at lower temperature[14]. Witoon et al[15] prepared a particular composition of CuO-ZnO-ZrO_2 on SZ by a co-precipitation method with different sulfur contents in order to produce methanol from CO_2. The effect of metal oxide composition has been investigated previously[16] for dehydration of methanol to dimethyl ether, and we found that 1% transition metal oxide could provide a good catalytic performance in terms of yield and stability. Furthermore, the influence of diffferent preparation methods[17] in the development of modified sulfated zirconia as catalysts for methanol conversion to DME and hydrocarbons is still desired.

The objective of our work was to demonstrate the impact of preparation method of 1%Mn metal incorporated SZ (impregnation and sol-gel techniques) on the morphology, distribution of the metal in the catalysts and their activities towards the convention of methanol. Then we studied the activity and stability of the catalyst under optimal conditions. The reaction mechanism was proposed based on evidence of the characterization for the used and regenerated catalyst.

1 Experiments

1.1 Catalyst preparation and characterization

The sulfated zirconia (SZ) catalyst was obtained according to a modified method of the sol-gel technique[8]. Zirconium isopropoxide (70%) was used as a precursor and isopropanol (99%) as a solvent, they were slowly mixed in one pot with H_2SO_4 (96%) with a Zr:S weight ratio of 1:0.038. The mixture was stirred for 30 min at room temperature. Hydrolysis and gelation were carried out for 1 h then dried at 120 °C for 12 h and calcined in static air at 600 °C for 3 h. 1%Mn was loaded onto SZ catalyst (Mn/SZ) via two techniques. Sol-gel technique, in which Zr precursor and $Mn(NO_3)_2{\cdot}6H_2O$ were added in the same step (Mn/SZ-S). Another technique was impregnation, where the Mn precursor was added after calcination of SZ powder, it was dried overnight, then calcined at 400 °C for 3 h (Mn/SZ-I). Catalysts structures were examined using an X-ray diffractometer (X0PERT PROMPD) with Cu *K*α radiation with a wavelength of $\lambda = 0.15406$ nm with a rating of 40 kV, 40 mA, step size = 0.02° and scan step time of 0.4 s in the range from 20°−80°. The chemical structures of all catalysts were conducted using a Fourier transform infrared (FT-IR) on the Nicolet iS10 FT-IR spectrometer in the range of 400−4000 cm^{-1}. The sulphur content was measured by the inductively coupled plasma atomic emission spectrometer (ICP). The specific surface area and pore size distribution were evaluated by N_2 adsorption-desorption isotherms using Quanta chrome Nova 3200 instrument that applies BET and BJH methods. The acidity of the catalysts was achieved by monitoring the amount of the desorbed NH_3 from the catalyst surface after exposure to NH_3 stream for a certain period. Surface morphology was examined by Scanning electron microscopy SEM images of model Joel 3500 electron microscope.

1.2 Catalytic activity measurements

The catalytic activities of SZ, sol-gel and impregnated catalysts for converting methanol to hydrocarbons were examined. The operations were performed in a conventional atmospheric fixed-bed quartz flow reactor using N_2 as a carrier gas at a constant flow rate of 40 mL/min. 0.5 g of the solid catalyst were mixed with glass beads and placed in the middle of the reactor with quartz wool to avoid hot spots and catalyst sintering. The catalyst was activated *in-situ* (1 h at 400°C under N_2 flow). The conversion was measured 1 h after the start of the reaction to ensure the equilibrium state. The collected liquid and gaseous products were analyzed using GC. First, the liquid hour space velocity (LHSV) of methanol was constant (0.05 h^{-1}) in a temperature range of 120−300 °C for all of the catalysts. The sol-gel catalyst was chosen for other activity and stability verification processes. LHSV ranged from 0.03 to 0.08 h^{-1} was investigated at 200 °C. Then, the TOS was tested up to 210 min at 200 °C and LHSV of 0.03 h^{-1}.

2 Results and discussion

2.1 Catalyst characterization

XRD patterns for SZ and *M*/SZ samples were illustrated in Figure 1(a). Peaks at 2° of 30°, 35°, 50°

and 60° indicated the tetragonal crystalline zirconia. As well known, the presence of sulfate ions in the zirconia matrix stabilizes the tetragonal phase when the SO_4^{2-} content is high enough to form a monolayer[18], where sulfate ions protect the surface from the adsorption of O_2 responsible for the tetragonal transition to monoclinic phase[19].

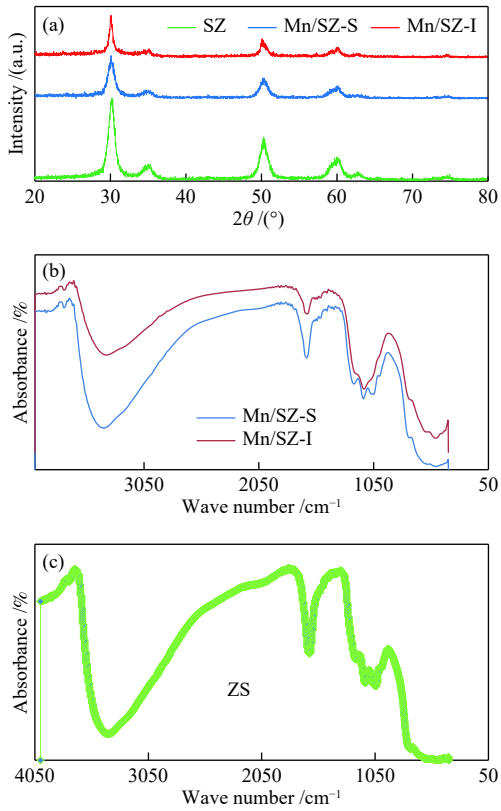

Figure 1　XRD patterns (a) and FT-IR spectra (b), (c) of the fresh catalysts

The metal incorporation didn't change the SZ structure and the intensities of the peaks were lower in *M*/SZ catalysts compared to the SZ catalyst, indicating the successful incorporation of the metal with a high absorption coefficient[20]. It was observed that the peaks at 35° and 60° split into two reflection peaks, confirming the tetragonal phase that has higher activity in catalytic reactions at low temperature range. The diffraction peaks of the metal oxide were not observed, indicating good dispersion on the surface of SZ[21]. It was noted that the crystallite size of Mn/SZ-I (27.8 nm) was greater than that of SZ (22.6 nm), while the Mn/SZ-S (13.3 nm) was approximately half the size of SZ (13.3 nm). The metal particles of Mn/SZ-I were randomly deposited on the surface of SZ, while those of Mn/SZ-S were buried in the pores and substituted in a zirconia lattice.

The typical FT-IR for SZ, Mn/SZ-S and Mn/SZ-I (Figure 1(b), 1(c)) showed diagnostic peaks at 450−760 cm^{-1} corresponded to the metal−oxygen bonding (Zr−O and Mn−O)[22]. The peak at 750 cm^{-1} which attributed to Zr−O vibration has shown in all catalysts but is somewhat sharper in SZ catalyst due to the absence of any other metal. The intense peak at 614 cm^{-1} indicated the presence of the tetragonal phase. The band at 1612 cm^{-1} was assigned to the δ_{O-H} vibration of the adsorbed water associated with sulfate groups[16]. For SZ catalyst, this peak had the greatest intensity indicating the highest acid sites number, whereas it was smaller in the impregnated catalyst than in the sol gel one because of the two calcination steps. On the other hand, several bands in the range of 900−1229 cm^{-1} assigned to S−O and S=O bonds of SO_4^{2-}, which indicated the presence of poly-sulfate species on the surface[23, 24]. The bands at 1139 and 1050 cm^{-1} were attributed to the bidentate sulfate ions that coordinate with Zr cations[20]. It is worth noting that peaks in this range appeared as one broadband in the Mn/SZ-I catalyst, whereas in Mn/SZ-S, these peaks were well separated into several peaks instead, although this catalyst has higher sulfur content than the impregnated one[15]. The exact sulfur contents were measured by ICP and found to be 4.8%, 4.2% and 3.9% for SZ, Mn/SZ-S and Mn/SZ-I, respectively. The large surface area of Mn/SZ-S (118.7 m^2/g) facilitated good dispersion of the acid sites in the bulk and on the surface, while the surface area was very small (33.2 m^2/g) in Mn/SZ-I that caused the accumulation of the acid sites in and out of the catalyst and appeared as a single peak in the FT-IR spectrum. Weak band was detected at 1400 cm^{-1} assigned to the S=O vibration mode. Band at 1340 cm^{-1} was observed only in Mn/SZ-S catalyst ascribed to the protonated oxygen (Zr−OH), this peak indicated stronger Brønsted acid sites than those of Mn/SZ-I[15]. Moreover, two bands were observed at 1517 and 1420 cm^{-1} over the Mn/SZ-S catalyst assigned to Brønsted and Lewis acid sites, respectively[25], where the band at 1509 cm^{-1} was attributed to the combination of both sites. The broadband at 3200 cm^{-1} was ascribed to the O−H stretching vibration mode of water associated with ZrO_2 which has increased by increasing the number of acid sites.

The N_2 adsorption-desorption isotherms for loaded SZ catalysts (not shown) reflected the effect of the preparation method on the surface area and the morphology of the catalysts. Mn/SZ-I showed type II

which is typical for microporous materials. Whereas, Mn/SZ-S exhibited type IV that corresponds to the mesoporous materials with H3 desorption hysteresis loop and slit the pores with wide range from 2 to 24 nm (Figure 2(a)). The specific surface area (SSA) for SZ was 111.8 m^2/g, which decreased to 33.2 m^2/g in the Mn/SZ-I catalyst, whereas it has increased to 118.7 m^2/g in Mn/SZ-S. Variation in surface area of Mn/SZ compared to SZ can be attributed to a modification of the catalyst structure due to the different techniques used during doping of Mn. This result was consistent with the crystallite sizes calculated from XRD. In the impregnation method, the surface area and pore volume decreased due to blocking of the pores with the randomly distributed metal oxide on the surface of SZ. However, in the sol-gel method the metal particles were substituted in the ZrO_2 matrix creating new pores and larger pore volume, thereby increasing the surface area. Yadav et al[26] pointed that, the difference in the surface area is due to the change in the sulfur contents on the catalyst surface caused by sulfate ions migration to the bulk of zirconia.

SEM images of the three catalysts were taken to clarify the surface morphology which supported the XRD and surface area observations (Figure 2(b)). The SEM pictures of the catalysts after loading with 1%Mn showed agglomerated and stuck irregular nanoparticles made the surface looked rough. The surface of the unloaded catalyst was white in color which turned to white yellow in 1%Mn/SZ-S and yellow in 1%Mn/SZ-I. This was attributed to the Mn ions which entered in the bulk of SZ in the sol gel method but in the impregnation method the most Mn metal was on the external surface of the catalyst. The surface structure of 1%Mn/SZ-I showed large particles with lower homogeneity than the unloaded catalyst which was compatible with the XRD results. On the other hand, the surface of 1%Mn/SZ-I appeared much coarser than 1%Mn/SZ-S. Also, the surface of Mn/SZ-S has spongy nature with more porosity than that of Mn/SZ-I catalyst.

The NH_3-TPD profiles for SZ and Mn/SZ were in the range of 100−900 °C (Figure 2(c)). The profile for SZ showed an intense sharp peak at 759 °C. It can be attributed to the NH_3 desorption from strong acid sites. This signal has the highest intensity among all catalysts (0.839 mmol/g), while the profile for Mn/SZ-I showed a sharp peak at 700 °C and a small peak at 773 °C with intensities of 0.184 and 0.066 mmol/g, respectively. Also, the Mn/SZ-S profile showed two broad peaks, the first one ranged from 110 to 400 °C with max. at 187 °C, assigned to weak Lewis acid sites, while the second at 814 °C corresponded to super acid sites. The total acidities of SZ, Mn/SZ-S and Mn/SZ-I were 0.839, 0.274 and 0.250 mmol/g, respectively, where the numbers of acid sites decreased significantly after loading with Mn metal[27]. It was also noted that the Mn/SZ-I catalyst has lower numbers of acid sites than those in Mn/SZ-S, indicating that the surface acid sites were masked by the impregnated metal. This result was consistent with FT-IR results. The acidity strength was affected after loading, where weaker acid sites were created due to interaction between sulfate groups and the metal oxide surface, also stronger acid sits were generated on the mixed oxide catalysts.

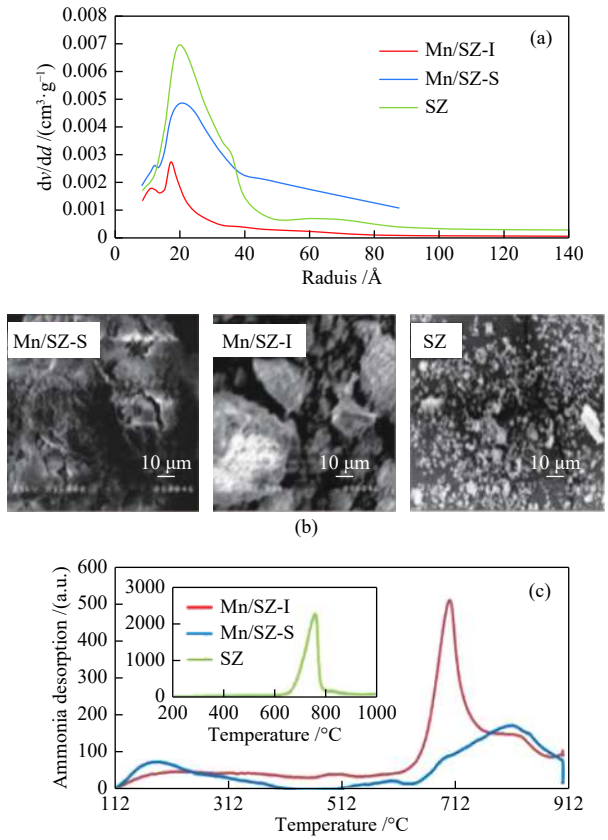

Figure 2 Pore size distribution (a), SEM images (b) and NH_3-TPD profiles (c) of the fresh catalysts

2.2 Catalytic activity results

The effective catalyst for converting methanol to DME should work at low temperature as possible. The effect of reaction temperatures (120−300 °C) on the catalytic activity of all catalysts was investigated (Figure 3). The total conversion increased with the reaction temperature. SZ catalyst had the lowest activity with 100%DME selectivity. This high

selectivity may be due to the presence of large numbers of acid sites compared to the other catalysts as observed in TPD analysis[21].

On the other hand, the promotion of SZ by Mn ions improved the catalytic activity. While, DME production decreased as the reaction temperature increased, paraffins, aromatics, and light olefins increased . This may be attributed to the masking of some strong acid sites by Mn metal ions that allowed another step in the conversion of DME to benzene or olefin. Therefore, the simple dehydration process was performed on the SZ catalyst, resulting in 100% DME production, while the deep dehydration mechanism could be carried out on the loaded catalysts that produced DME and hydrocarbons[17, 28−31]. The higher selectivity of DME on Mn/SZ-S catalyst than that on Mn/SZ-I can be attributed to the large surface area and higher acidity. Aromatic/paraffinic hydrocarbons were produced at 200 °C using Mn/SZ catalysts with small selectivity, which increased at higher temperatures. This may be due to the presence of basic sites (metal oxide) which accelerated the dehydration of DME to light olefin and aromatics. Using Mn/SZ-S catalyst (LHSV of 1 mL/min (0.03 h^{-1})), the selectivity toward DME increased up to 180°C and then declined (Figure 3(b)), while the production of light olefins and aromatics increased continually. It was noted that the formation of the aromatic is preferable compared to light olefins at all temperature range. Thermodynamically, olefins was favored in high temperature range only at low methanol conversion[32].

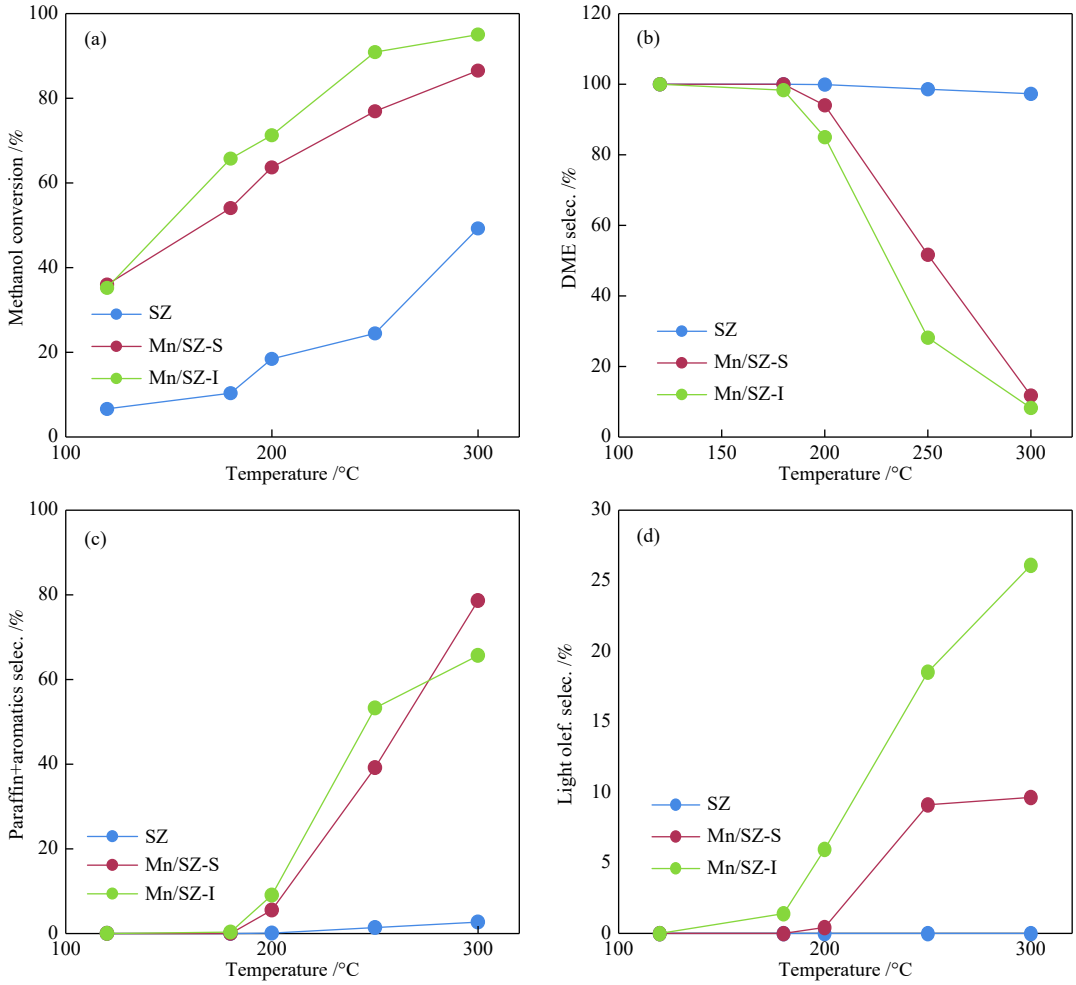

Figure 3　Variation of methanol conversion with temperature (a), selectivity of DME (b), aromatics (c) and olefins (d) (t = 120−300 °C, LHSV = 0.03 h^{-1})

Activity results of Mn/SZ-S showed total conversion of 62.87% and high yield of DME (59.87%) with selectivity of 95.23% at 200 °C. So, the methanol conversion as a function of LHSV was studied on Mn/SZ-S as a selected catalyst at 200 °C. It can be seen that total conversion gradually decreased from 78.60% to 67.67% with an increase in LHSV from 0.5 to 2.5 mL/min (0.02−0.08 h^{-1}) (Figure 4(a)), which attributed

to the decrease in the reactant residence time. Also, DME was the main product that decreased from 62.48% to 51.58% with increased LHSV.

Figure 4(b) showed methanol conversion and product distribution with time (30−210 min) at 200 °C and LHSV of 0.02 h^{-1} (0.5 mL/min). As can be seen, 120 min was the maximum time on stream for the catalyst after which the catalyst started to deactivate.

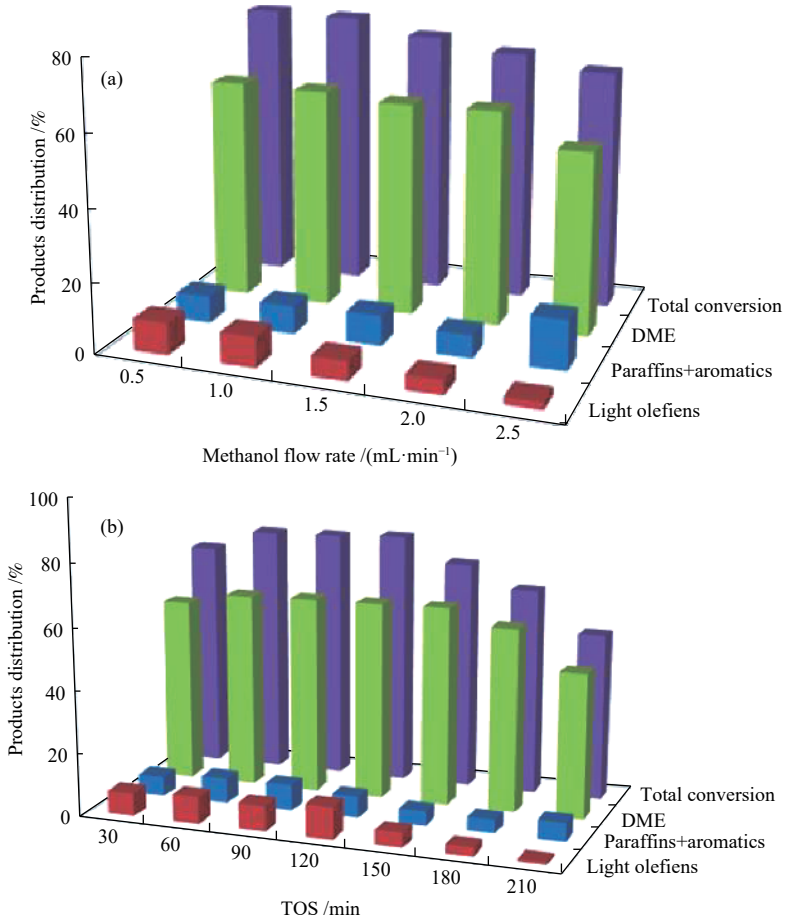

Figure 4 The product distribution of methanol conversion as a function of LHSV (a), time (b) on the Mn/SZ-S catalyst

The structure of the used Mn/SZ-S catalyst was examined as an additional study, and this was done by comparing the XRD patterns of fresh and used Mn/SZ-S catalysts (Figure 1(a) and Figure 5). We found that the crystalline zirconia peaks in the fresh catalyst were the only observable peaks, while the intensity of these peaks decreased significantly in the used one. Sohn et al[31] assumed that there was an interaction between zirconium sulfate and the ZrO_2 surface, delaying the crystallization of ZrO_2. We assumed from the broadening of the peaks that the crystalline size of the used catalyst was greater than that of the fresh one. Moreover, the pattern clearly showed the presence of the orthorhombic phase of $Zr(SO_4)_2$ at 20.5°, 22.7°, 24.6°, 26.2°, and 29.7°. Testa et al[32] assumed that the electron density in $Zr(SO_4)_2$ shifted from Zr atom towards the sulfate group, leading to a higher Lewis acidity, so it would affect the catalyst activity.

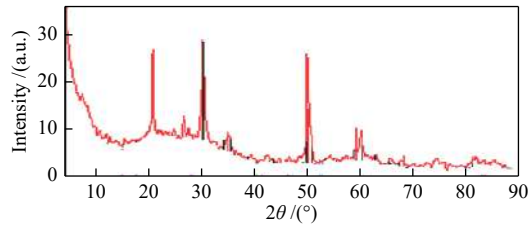

Figure 5 XRD patterns of the used Mn/SZ-S catalyst

The stability of the Mn/SZ-S catalyst was investigated. The used catalyst was regenerated by burning it in a flow of air at 500 °C for 1 h to breakdown any hydrocarbons on the surface. Four methanol conversion cycles were performed at optimum condition of 200 °C and LHSV of 0.02 h^{-1} within 1 h. There was a significant decrease in total conversion; 47.67%, 36.85%, 29.20% and 28.90%, respectively, from the first to the fourth cycle (Figure 6(a)); that referred to the decrease in the total acidity. Testa et al[32] reported that the hydrolysis of zirconium sulfate to H_2SO_4 and $Zr(OH)_4$ leached the sulfate groups, reducing the

catalyst acidity. This illustratesd the catalytic deactivation mechanism, as DME, light olefins, and parafins + aromatics decreased from cycle 1 to cycle 3 (from 20.97%, 21.90%, 2.90% to 13.75%, 8.65%, 1.951%, respectively), then DME in the fourth cycle increased to 14.75% while other hydrocarbons decreased. This indicated that strong acid sites have been covered with adsorbed carbonaceous products and have blocked pores. Although catalytic activity decreased, DME selectivity increased from the first cycle to the fourth cycle (but still lower than that of the fresh catalyst). This result may be associated with a decrease in the acidity of the catalyst due to the leaching of sulfate groups during the reaction. Also, it may be due to blocking of strong acid sites associated with deep dehydration that led to high hydrocarbons, while remaining weak and medium acid sites suitable for the simple dehydration that produces DME[17]. This was demonstrated by studying the characterization of the reused Mn/SZ-S catalyst after the fourth cycle. The FT-IR spectrum of the used Mn/SZ-S catalyst after 4 cycles was illustrated in Figure 6(b).

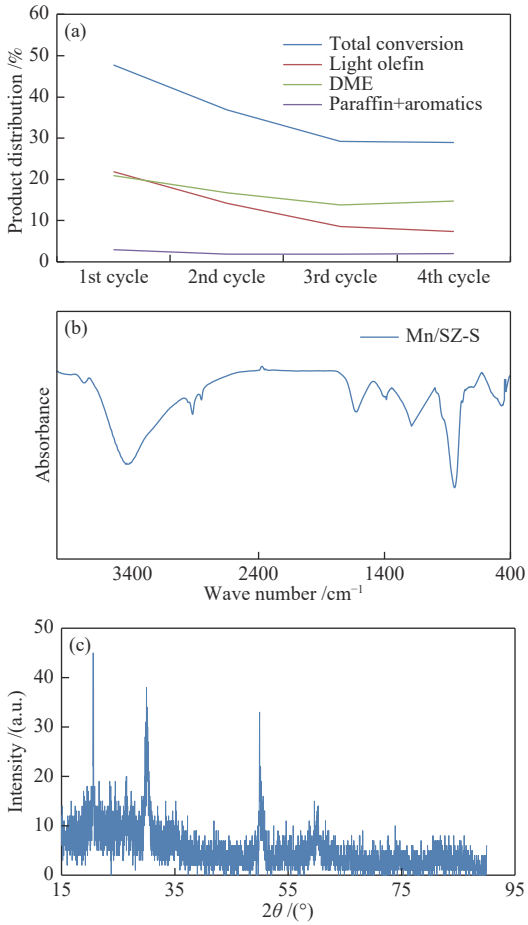

Figure 6　Reusability of the catalyst (react. cond.: t = 200 ℃; LHSV = 0.03 h^{-1}; after 1 h) (a), FT-IR (b) and XRD (c) of the Mn/SZ-S catalyst after four cycles

Bands at approximately 2858, 2927, and 2965 cm^{-1} were attributed to paraffins, where Popova et al[17], confirmed that the bands in this region indicated the formation of long chain hydrocarbons on Brönsted acid sites. We noted that the bands ranging between 450−760 cm^{-1} decreased significantly. Also, the band at 614 cm^{-1} in the fresh catalyst indicated the presence of the tetragonal zirconia (t-ZrO_2) disappeared in the used one after four cycles. This result was compatible with the XRD result for the used and the regenerated catalyst. The intense peak at 850 cm^{-1} was related to SiC as inert material (to increase the catalyst amount). The band at approximately 1400 cm^{-1} assigned to the S=O bond in the sulfate group clearly appeared in the regenerated catalyst. This indicated a low coverage of protonated sulfate on the surface[20]. XRD of the used catalyst after four cycles showed the disappearance of all peaks belonged to $Zr(SO_4)_2$ due to the decomposition of sulfate groups which explained the decrease in the activity of the catalyst (Figure 6(c)).

In comparison to some other available researches, the prepared catalysts performed very well during this study. Our results are comparable in this condition to other transition metal SZ catalysts described in many previous literatures. Hussain et al[33] prepared SZ and silica doped SZ catalysts for methanol conversion to DME and HC using a high pressure batch reactor. The reaction temperature and the pressure were between 100 and 200°C and from 260 to 575 psig, respectively. The methanol conversion was 41% and 43% on SZ and Si/SZ with DME selectivity of 6% an 0.4%, respectively. In another study, sulfated zirconia was mixed with CuO-ZnO-ZrO_2 for direct synthesis of DME from CO_2 hydrogenation[15]. The maximum DME yield was 3.6% at 260 °C and 20 bar and the total CO_2 conversion to oxygenated compounds was 4%. In 2018, Said et al[16] investigated the dehydration of methanol to dimethyl ether using different metal sulfate on zirconia treated with 10%SO_4^{2-}. The results revealed that, 6.5%Cu/SZ showed the best activity with maximum yield of DME about 87% at 275 °C and atmospheric pressure. Palomo et al[34] prepared Zr-loaded P-containing activated carbon (0.75%−7.5%). The methanol conversion was 69% and the selectivity towards DME was 95% using 5% Zr loaded catalyst. Although the DME production is quite high; it was obtained at a temperature as high as 400 °C. Recently, in 2020, zirconium transition metal phosphates M = Ni, Cu, Mn; $0 \leqslant x \leqslant 0.5$) have been tested for methanol

conversion[35]. The temperature range was 200−450 °C. Ni and Cu modified catalysts exhibited the highest conversion (up to 95%) and DME selectivity which was comparable to that on available commercial catalysts. In comparison to the above mentioned results, the catalysts utilized in this study have been prepared via simple methods with small amount of transition metal at room temperature. They have shown better performance compared to other prepared catalysts. The enhanced conversion and selectivity achieved during this work can be ascribed to the quality of the structure of the loaded catalyst in terms of the high surface area, as well as the suitable concentration and strength of the acid sites.

3 Conclusions

The effects of adding 1%Mn to SZ by sol gel (Mn/SZ-S) and impregnation (Mn/SZ-I) on the methanol conversion process were tested. The Mn/SZ-S catalyst has the best catalytic performance. The results showed high total conversion of 74.26% and 63.54% yield of DME at 200°C and 0.03 h^{-1} LHSV. The high catalytic activity was attributed to the large surface area and the high acidity. The XRD pattern of the used catalyst showed that the presence of zirconium sulfate resulted in a high Lewis acidity. Furthermore, the interaction between zirconium sulfate and zirconia improved the physicochemical properties of the catalyst. The highest activity for the Mn/SZ-S catalyst was detected at optimum conditions of 200°C and 0.02 h^{-1}, while the maximum TOS was detected at 120 min after which the catalyst began to deactivate. The stability of the Mn/SZ-S catalyst was verified during 4 cycles at the optimum conditions. XRD and FT-IR analysis highlighted the deactivation mechanism of the regenerated catalyst after the forth cycle. As, the crystallinity of zirconia decreased and the sulfate groups were also leached, the carbonaceous products blocked the acid sites and the the pores of the catalyst.

References

[1] SOLYMAN S M, ABOUL-GHEIT N A K, TAWFIK F M, SADEK M, AHMED H A. Performance of ultrasonic - treated nano-zeolites employed in the preparation of dimethyl ether[J]. Egypt J Pet, 2013, **22**: 91−99.

[2] SOLYMAN S M, ABOUL-GHEIT N A K, SADEK M, TAWFIK F M, AHMED H A. The effect of physical and chemical treatment on nano-zeolite characterization and their performance in dimethyl ether preparation[J]. Egypt J Pet, 2015, **24**: 289−297.

[3] ABOUL-FOTOUH S M K, ALI L I, NAGHMASH M A, ABOUL-GHEIT N A K. Effect of the Si/Al ratio of HZSM-5 zeolite on the production of dimethyl ether before and after ultrasonication[J]. J Fuel Chem Technol, 2017, **45**(5): 581−588.

[4] ABOUL-GHEIT A K, ABOUL-FOTOUH S M, ALI L I, NAGHMASH M A. Ultrasonication of H-MOR zeolite catalysts for dimethylether (DME) production as a clean fuel[J]. J Pet Technol Altern Fuels, 2014, **5**(2): 13−25.

[5] ABOUL-FOTOUH S M, ABOUL-GHEIT N A K, NAGHMASH M A. Dimethylether production on zeolite catalysts activated by Cl^-, F^- and/or ultrasonication[J]. J Fuel Chem Technol, 2016, **44**(4): 428−436.

[6] SOLYMAN S M, BETIHA M A. The performance of chemically and physically modified local kaolinite in methanol dehydration to dimethyl ether[J]. Egypt J Pet, 2014, **23**: 247−254.

[7] RADWAN D, SAAD L, MIKHAIL S, SELIM S A. Catalytic evaluation of sulfated zirconia pillared clay in N-hexane transformation[J]. J Appl Sci Res, 2009, **5**(12): 2332−2342.

[8] IBRAHIM A H, ISMAIL H A S, EL-DESOUKI D S, ABDEL-AZIM S A, ABOUL-GHEIT N A K. Preparation of sulfated zirconia catalyst loaded by copper in "nano-scale: Green application to synthesis of biolubricant[J]. Egypt J Chem, 2018, **61**: 503−516.

[9] LIU N, WANG X, SHI L, MENG X. Metallic oxide-modified sulfated zirconia: an environment-friendly solid acid catalyst[J]. New J Chem, 2019, **43**(8): 3625−3632.

[10] FÖTTINGER K, HALWAX E, VINEK H. Deactivation and regeneration of Pt containing sulfated zirconia and sulfated zirconia[J]. Appl Catal A: Gen, 2006, **301**: 115−122.

[11] KEDIA A O, ZAIDI H A. Conversion of methanol to hydrocarbons over Ni-ZSM-5 catalyst[J]. Int J Adv Res Sci Eng Technol, 2014, **3**(1): 350−356.

[12] ABOUL-GHEIT A K, GAD F K, ABDEL-ALEEM G M, EL-DESOUKI D S, ABDEL-HAMID S M, GHONEIM S A, IBRAHIM A H. Pt, Re and Pt-Re incorporation in sulfated zirconia as catalysts for n-pentane isomerization[J]. Egypt J Pet, 2014, **23**: 303−314.

[13] SOYLU G S P, ISIK A B, BOZ I. Dehydroisomerization of n-butane over metal promoted sulfated zirconia[J]. Turkish J Eng Env Sci, 2009, **33**: 273−279.

[14] HSU C Y, HEIMBUCH C R, ARMES C T, GATES B C. A highly active solid superacid catalyst for n-butane isomerization: a sulfated oxide containing iron, manganese and zirconium[J]. J Chem Soc, Chem Comm, 1992: 1645−1646.

[15] WITOON T, PERMSIRIVANICH T, KANJANASOONTORN N, AKKARAPHATAWORN C, SEUBSAI A, FAUNGNAWAKIJ K, WARAKULWIT C, CHAREONPANICH M, LIMTRAKUL J. Direct synthesis of dimethyl ether from CO_2 hydrogenation over Cu-ZnO-ZrO_2/SO_4 2--ZrO_2 hybrid catalysts: Effects of sulfur-to-zirconia ratios[J]. Catal Sci Technol, 2015, **5**: 2347−2357.

[16] SAID A E A A, EL-AAL M A. Effect of different metal sulfate precursors on structural and catalytic performance of zirconia in dehydration of

methanol to dimethyl ether[J]. J Fuel Chem Technol, 2018, **46**(1): 67−74.

[17] POPOVA M, SZEGEDI Á, LAZAROVA H, DIMITROV M, KALVACHEV Y, ATANASOVA G, RISTIĆ A, WILDE N, GLÄSER R. Influence of the preparation method of sulfated zirconia nanoparticles for levulinic acid esterification[J]. React Kinet Mech Catal, 2017, **120**: 55−67.

[18] CHEN W H, KO H H, SAKTHIVEL A, HUANG S J, LIU S H, LO A Y, TSAI T C, LIU S B. A solid-state NMR, FT-IR and TPD study on acid properties of sulfated and metal-promoted zirconia: Influence of promoter and sulfation treatment[J]. Catal Today, 2006, **116**: 111−120.

[19] SRINIVASAN R, WATKINS T R, HUBBARD C R, DAVIS B H. Sulfated zirconia catalysts. the crystal phases and their transformations[J]. Chem Mater, 1995, **7**: 725−730.

[20] SHI G L, YU F, YAN X L, LI R F. Synthesis of tetragonal sulfated zirconia via a novel route for biodiesel production[J]. J Fuel Chem Technol, 2017, **45**(3): 311−316.

[21] SOHN J R, LIM J S. Catalytic properties of $NiSO_4/ZrO_2$ promoted with Fe_2O_3 for acid catalysis[J]. Mater Res Bull, 2006, **41**: 1225−1241.

[22] BENITO H E, ALAMILLA R G, ENRÍQUEZ J M H, DELGADO F P, GUTIÉRREZ D L, GARCÍA P. Porous silicates modified with zirconium oxide and sulfate ions for alcohol dehydration reactions[J]. Adv Mater Sci Eng, 2015, **2015**: 1−11.

[23] REN K, KONG D, MENG X, WANG X, SHI L, LIU N. The effects of ammonium sulfate and sulfamic acid on the surface acidity of sulfated zirconia[J]. J Saudi Chem Soc, 2019, **23**: 198−204.

[24] VLASOV E A, MYAKIN S V, SYCHOV M M, AHO A, POSTNOV A Y, MAL'TSEVA N V, DOLGASHEV A O, OMAROV S O, MURZIN D Y. On synthesis and characterization of sulfated alumina-zirconia catalysts for isobutene alkylation[J]. Catal Lett, 2015, **145**: 1651−1659.

[25] VAHID B R, SAGHATOLESLAMI N, NAYEBZADEH H, MASKOOKI A. Preparation of nano-size Al-promoted sulfated zirconia and the impact of calcination temperature on its catalytic activity[J]. Chem Biochem Eng Q, 2012, **26**(2): 71−77.

[26] YADAV G D, MURKUTE A D. Preparation of a novel catalyst UDCaT-5: Enhancement in activity of acid-treated zirconia - Effect of treatment with chlorosulfonic acid vis-à-vis sulfuric acid[J]. J Catal, 2004, **224**: 218−223.

[27] BENOMAR S, MASSÓ A, SOLSONA B, ISSAADI R, NIETO J L. Vanadium supported on alumina and/or zirconia catalysts for the selective transformation of ethane and methanol[J]. Catalysts, 2018, **8**: 126.

[28] MA T, IMAI H, YAMAWAKI M, TERASAKA K, LI X. Selective synthesis of gasoline-ranged hydrocarbons from syngas over hybrid catalyst consisting of metal-loaded ZSM-5 coupled with copper-zinc oxide[J]. Catalysts, 2014, **4**: 116−128.

[29] MORADI G R, YARIPOUR F, VALE-SHEYDA P. Catalytic dehydration of methanol to dimethyl ether over mordenite catalysts[J]. Fuel Process Technol, 2010, **91**: 461−468.

[30] STÖCKER M. Methanol-to-hydrocarbons: Catalytic materials and their behavior[J]. Microporous Mesoporous Mater, 1999, **29**: 3−48.

[31] SOHN J R, LEE D G. Characterization of zirconium sulfate supported on TiO_2 and activity for acid catalysis[J]. Korean J Chem Eng, 2003, **20**: 1030−1036.

[32] TESTA M, LA PAROLA V, MESRAR F, OUANJI F, KACIMI M, ZIYAD M, LIOTTA L. Use of zirconium phosphate-sulphate as acid catalyst for synthesis of glycerol-based fuel additives[J]. Catalysts, 2019, **9**: 148.

[33] HUSSAIN S T, MAZAR M, GUL S, CHUANG K T, SANGER A R. Dehydration of methanol to dimethyl ether, ethylene and propylene over silica-doped sulfated zirconia[J]. Bull Korean Chem Soc, 2006, **27**(11): 1844−1850.

[34] PALOMO J, RODRIGUEZ-MIRASOL J, CORDERO T. Methanol dehydration to dimethyl ether on Zr-loaded P-containing mesoporous activated carbon catalysts[J]. Materials, 2019, **12**: 2204−2220.

[35] GLUKHOVA I O, ASABINA E A, PET'KOV V I, MIRONOVA E Yu, ZHILYAEVA N A, KOVALSKII A M, YAROSLAVTESEV A B. Zirconium d-transition metal phosphates as catalysts for selective dehydration of methanol to dimethyl ether[J]. Inorg Mater, 2020, **56**(4): 395−401.